Physics and Chemistry of the Earth 34 (2009) 309–315

Contents lists available at ScienceDirect

Physics and Chemistry of the Earth

journal homepage: www.elsevier.com/locate/pce

Delineation of small reservoirs using radar imagery in a semi-arid environment: A case study in the upper east region of Ghana

F.O. Annor [a,b,*], N. van de Giesen [c], J. Liebe [d], P. van de Zaag [a,c], A. Tilmant [b], S.N. Odai [b]

[a] Department of Management and Institutions, UNESCO–IHE, Westvest 7, Delft, The Netherlands
[b] Department of Civil Engineering, Kwame Nkrumah University of Science and Technology, Kumasi, Ghana
[c] Water Resources Section, Delft University of Technology, Stevinweg 1, 2628 CN Delft, The Netherlands
[d] Department of Biological and Environmental Engineering, Cornell University, 76 Riley–Robb Hall, Ithaca, NY 14853–5701, USA

ARTICLE INFO

Article history:
Received 28 November 2007
Received in revised form 29 July 2008
Accepted 21 August 2008
Available online 5 September 2008

Keywords:
ENVISAT ASAR
Small reservoirs
Radar
Ghana

ABSTRACT

Small reservoirs serve many people living in semi-arid environments. Water stored in these reservoirs is used to supplement rainfed agriculture, allow for dry season irrigated agriculture and ensure the availability of water for domestic purposes. In order to manage the water effectively for competing uses, the actual storage of these reservoirs needs to be known. Recent attempts to delineate these reservoirs using remote sensing with Landsat imagery have been successful, especially in the upper east region of Ghana, West Africa.

This paper shows that radar images (ENVISAT ASAR) can be used to provide similar information all year-round. Radar images have as an important advantage that they are not impaired by cloud cover and thus can be used during the rainy season. Another advantage of radar images is that images taken during night time are usable. The paper compares satellite derived data with field measurements of 21 small reservoirs. Whereas ENVISAT images on the average tend to overestimate the surface areas of small reservoirs, in certain reservoirs these areas are systematically under-estimated due to the shallow tail-ends of reservoirs that tend to have reed vegetation. These cannot be readily distinguished from the surrounding vegetation outside the reservoirs. This paper therefore provides a proof of concept of the monitoring of small reservoir volumes by radar imagery.

1. Introduction

In periods of drought, the rural population in most semi-arid environments rely heavily on small reservoirs to sustain their livelihoods (Liebe et al., 2005; Poolman et al., 2006; Balazs, 2006; Faulkner et al., 2008). In this context, small reservoirs are defined as reservoirs with surface areas of less than 100 hectares. Water stored in these reservoirs allows for all year-round irrigated agriculture and ensures that domestic water shortages are reduced during dry periods. In order to manage the water effectively for competing uses, the actual storage of these reservoirs need to be accurately estimated. Landsat imagery has been used recently to delineate some of the reservoirs in the upper east region (UER) of Ghana, West Africa (Liebe et al., 2005), Zimbabwe (Sawunyama et al., 2005) and India (Mialhe et al., 2008). The accuracy of the lateral delineation of these reservoirs with Landsat was very good. However, Landsat images and images obtained from similar optical sensors are affected by cloud cover especially during the rainy season (Van de Giesen, 2000; Xu et al., 2004; Liebe et al., 2005).

This research focuses on how radar images from the ENVISAT advanced synthetic aperture radar (ENVISAT ASAR) can be used to provide all year-round monitoring. Radar has two important advantages relevant for this study, namely that it is independent of cloud cover (Horritt and Mason, 2001; Herold et al., 2004) and that observations can be made during night time. The goal of this research is to use radar imagery to quantify the actual volume of water stored in reservoirs, partially to overcome the fact that there is limited availability of ground data. This information may be used to enhance decision making especially for irrigation scheduling and water allocation in Ghana.

2. Description of the study area

The upper east region (UER), shown in Fig. 1, covers about 3.7% (8842 sq kms) of the landmass of Ghana. Rainfall over the past 40 years has averaged 1044 mm/a which is suitable for a single wet season crop (IFAD, 2007). Mean annual temperature of 28 °C. The mean annual rate of pan evaporation is 2540 mm/a (Gyau-Boakye and Tumbulto, 2006). The upper east region has a mean population

* Corresponding author. Address: Department of Civil Engineering, Kwame Nkrumah University of Science and Technology, Kumasi, Ghana. Tel.:/fax: +233 51 602 35.
E-mail address: annorfrank@yahoo.co.uk (F.O. Annor).

1474-7065/$ - see front matter © 2008 Elsevier Ltd. All rights reserved.
doi:10.1016/j.pce.2008.08.005

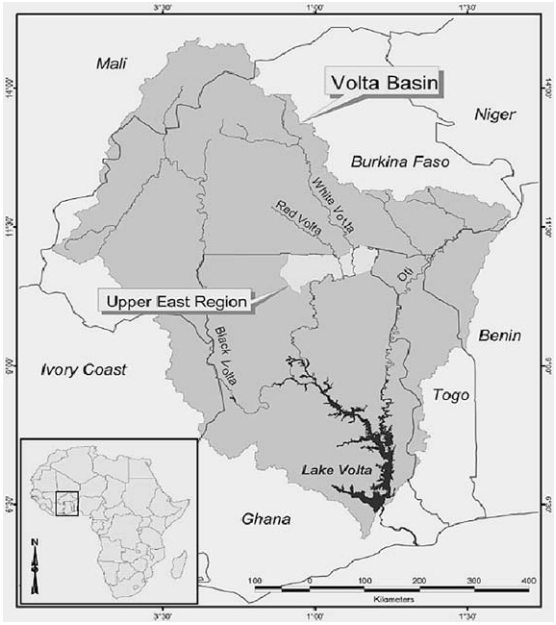

Fig. 1. The upper east region of Ghana within the Volta Basin (Adapted from Liebe et al., 2005).

density of 125 inhabitants/km^2 (IFAD, 2007). Crop and livestock farming is the main economic activity. The natural land cover is an open park savannah of grass with scattered trees. Presently, most of the UER is cultivated. Crops include rice, maize, millet, sorghum and vegetables. Access to water for livestock, fishery, irrigation and domestic uses during the dry season is a major concern for the population.

The Ghana poverty reduction strategy paper (GPRSP, 2005) identifies northern Ghana as the number one poverty endemic area in Ghana. In 1986, it was estimated that 67% of small holders (those farming less than 1.6 ha and in the UER 2.4 ha) in Ghana were living in poverty (IFAD, 2007). This was a major justification for the government in 1998 to launch a land conservation and smallholder rehabilitation project (LACOSREP) that would provide farm families with adequate supplies of irrigation water. The rehabilitation of existing small dams or reservoirs and the formation and strengthening of water users associations are key activities of this programme.

In the UER the wet period is relatively short and is further marked by variations in arrival time, duration and intensity of rainfall. This creates inter-year variations in agricultural production potential (IFAD, 2007). In turn, this explains the reliance of smallholder farmers on small reservoirs which often is the only source of water available for dry-season crops.

Accurate estimation of the actual volume of water stored in reservoirs at regular time intervals (e.g. monthly) is important for effective planning and management. Knowledge of the storage volume would enable the relevant agencies, including the irrigation development authority (IDA) and the ministry of food and agriculture (MOFA), to advise farmers on the type of crops to grow. Most of the reservoirs in the UER were built by different agencies and are mainly managed by MOFA, IDA and the district assemblies. These institutions find it difficult to continuously monitor the status of these small reservoirs due to lack of resources and inadequate human capacity. Their reliance on ground surveys to estimate actual storage volumes turns out to be time-consuming and prohibitively expensive and hence the institutions are unable to monitor the storage in the reservoirs themselves. This research demonstrates the possibility of monitoring water storage in small reservoirs all year round by remote sensing using satellite imagery from ENVISAT ASAR.

3. Materials and methods

3.1. Delineation of reservoirs by remote sensing using passive and active sensors

The infrared, visible red and near-infrared bands found in Landsat/TM and similar satellite imagery is used to distinguish between land and water and map the extent of open water surface (Toyra et al., 2002; Liebe et al., 2005). In Landsat ETM+, bands 4–7 (infrared) are used to distinguish between water and vegetation. Water, when not turbulent, absorbs energy in the near-infrared and infrared wavelengths hence appear darker in the imagery whereas land and vegetation are seen as bright spots. The techniques used for the delineation of open water range from visual interpretation by density slicing and band–ratio-approaches such as the normalised difference water index (NDWI) to different methods of supervised and unsupervised classification (Liebe, 2002).

As mentioned earlier on, cloud cover and the presence of reeds and other suspended organic and inorganic materials on the surface of reservoirs makes it difficult to distinguish between land and water using Landsat. This suggests the use of ENVISAT ASAR imagery, which is weather independent, as a possible alternative for, or complement to, Landsat imagery.

ENVISAT ASAR is a follow up of ERS-1 and ERS-2 satellites. It is on board the ENVISAT satellite which is operated by the European Space Agency (ESA) and was launched from Kourou in French Guiana on 1st March, 2002. The ENVISAT ASAR uses the C-band (5.331 GHz). Outgoing and incoming signals can be like-polarized; both horizontal (HH) or both vertical (VV). Alternatively, outgoing and incoming signals can be cross-polarized (VH or HV). ENVISAT can be programmed to acquire images in dual-polarization mode. In that case, scenes can be imaged simultaneously with two of the possible polarization combinations. For this study, we used dual polarization mode as this mode was anticipated to have advantages over single polarized images. ENVISAT ASAR has a temporal resolution of 35 days and a spatial resolution of 30 m.

3.2. Lateral delineation of reservoirs

For this research, six ENVISAT SLC alternating polarization mode data were acquired in the framework of ESA's Tiger program. The description of the data is given in Table 1. In this study, the magnitude of the polarization channels (C-HH and C-HV) was used for the classification of land and water. The channels were also combined to study their ability to enhance the land/water contrast in the images.

The single look complex (SLC) images were imported into ERDAS Imagine software. Radar images often have lots of speckles or noise; this was reduced with the gamma-map filter (Fig. 2). Many filters like Lee, Lee-Sigma and Frost assume that the noise is Gaussian distributed. Studies conducted recently especially on natural vegetated areas have proven that a gamma distribution is

Table 1
Description of Envisat ASAR data used to develop the model

No	Product	Swath	Date	Resolution (m)
1	ASA_APH	I1	6/1/07	12
2	ASA_APH	I4	9/1/07	10
3	ASA_APH	I1	22/1/07	12
4	ASA_APH	I2	25/1/07	11
5	ASA_APH	I4	28/1/07	10
6	ASA_APH	I7	31/1/07	7.5

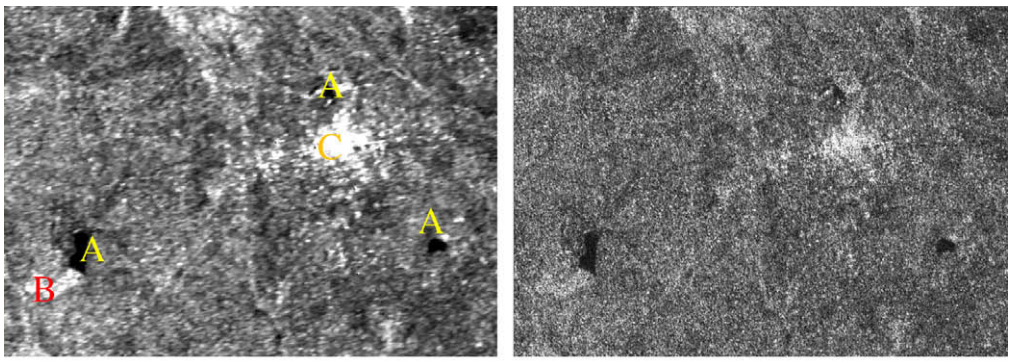

Fig. 2. C-HH backscatter of a SLC image, 31st January, 2007. The image shows three small reservoirs (A), an irrigated area (B), and a village (C). The remainder consists of sparse trees with dried grasses and crops residues.

more appropriate. The Maximum A Posteriori (MAP) filter assumes that the original pixel digital number (DN) lies between the local average and the degraded (actual) pixel DN. It then attempts to estimate the original pixel DN based on this assumption. The algorithm, which was developed by Frost et al. (1982) as cited in the ERDAS field guide (2005), is built on the cubic equation given by

$$\hat{I}^3 - \bar{I}\hat{I}^2 + \sigma(\hat{I} - \mathrm{DN}) = 0 \quad (1)$$

where

- $\hat{I}$ = Sought value
- $\bar{I}$ = Local mean
- σ = Original image variance
- DN = Input value

To reduce the speckle noise, the images were filtered with a 7×7 followed by a 5×5 window gamma-map adaptive filter. Other filters such as mean, median, Lee-sigma and local region did not produce satisfactory results in terms of speckle reduction and detail preservation. Fig. 2 shows the unfiltered and filtered images of the same scene. In most cases the C-HH polarization combination was used.

After filtering the images, they were geocoded to UTM, Zone 30 N, using the WGS84 ellipsoid. The images were georeferenced in ArcMap using 2nd order polynomial (affine) transformation with an RMS error of about 20 m with 15 ground control points. The images were subsequently classified using a hybrid (a combination of unsupervised and supervised) maximum likelihood classification with training sites verified with ground truth data in ERDAS Imagine. The maximum likelihood classifier calculates for each class the probability of a cell belonging to that class given its attribute values. The cell is then assigned to the class with the highest probability. Fig. 3 shows a un-georeferenced and a georeferenced image (the images are unclassified and are from the same scene). The magnitude of the C-HH or in other cases the C-HV polarized channel was used to delineate the reservoirs. A combination of the two channels especially when one is good and the other bad did not yield good results hence only one was used at a time. The delineation was performed through an on-screen digitization in ArcMap. Automatic delineation did not yield good results due to the noise in the imagery that remained despite filtering.

3.3. Measuring the outline of reservoirs on the ground

Ground truthing was carried out from 31st January to 7th February, 2007 at the time of overpass of the satellite. Forty-two dams were visited (Fig. 4). The outlines were obtained with a Garmin 76 GPS instrument, with an accuracy of <15 m RMS 95% typical. Field work was carried out in the dry season (November–April) hence the reservoirs were not at maximum capacity at the time of visit. Some of the reservoirs were free of reeds; however most of them had reeds at the tail-end with some having more than 40% of their surface area covered with reeds. Fig. 4 shows a reservoir with reeds on its surface.

The outlines of the reeds on the surface of the reservoirs were taken with the GPS and a rubber boat. The data stored on the GPS was imported into GPS Trackmaker13. This was used to convert the GPS data into text formats so it could be read by ArcCatolog. The points were connected together to form polygons. The surface areas and perimeter were then calculated.

3.4. Bathymetric survey

A bathymetric survey was carried out on 14 reservoirs using an echo-sounder and a telescopic stadia rod. The collection of depth data did not follow any predefined grid. Each reservoir was surveyed taking into consideration the local variations and characteristics, such as side arms, asymmetric basin shapes, etc. On-shore fixed points such as trees, rocks, houses, etc., were used to roughly gauge positioning within the reservoir and to row in approximately straight lines along which measurements were taken. The echo-sounder measures depth and corresponding GPS points in a continuous stream. To derive the reservoirs' storage volumes, the field measurements were processed and translated into 3-D models. These models were used to obtain area and volume at varying depths from full supply to when the reservoir is completely emptied or dried up.

4. Results and discussion

4.1. Correlation between field and satellite measured reservoir surface areas

Table 2 provides the wet surface area of 18 reservoirs obtained from the field survey and from satellite images. These reservoirs were selected such that they covered the entire study area. These were used to model the correlation between the field and satellite derived areas.

The normalized difference area index (NDAI) adapted from Liebe (2002) and the deviation area index (DAI) adapted from Sawunyama et al. (2005) were used to compare the surface area measured by satellite and in the field. NDAI and DAI are defined as follows

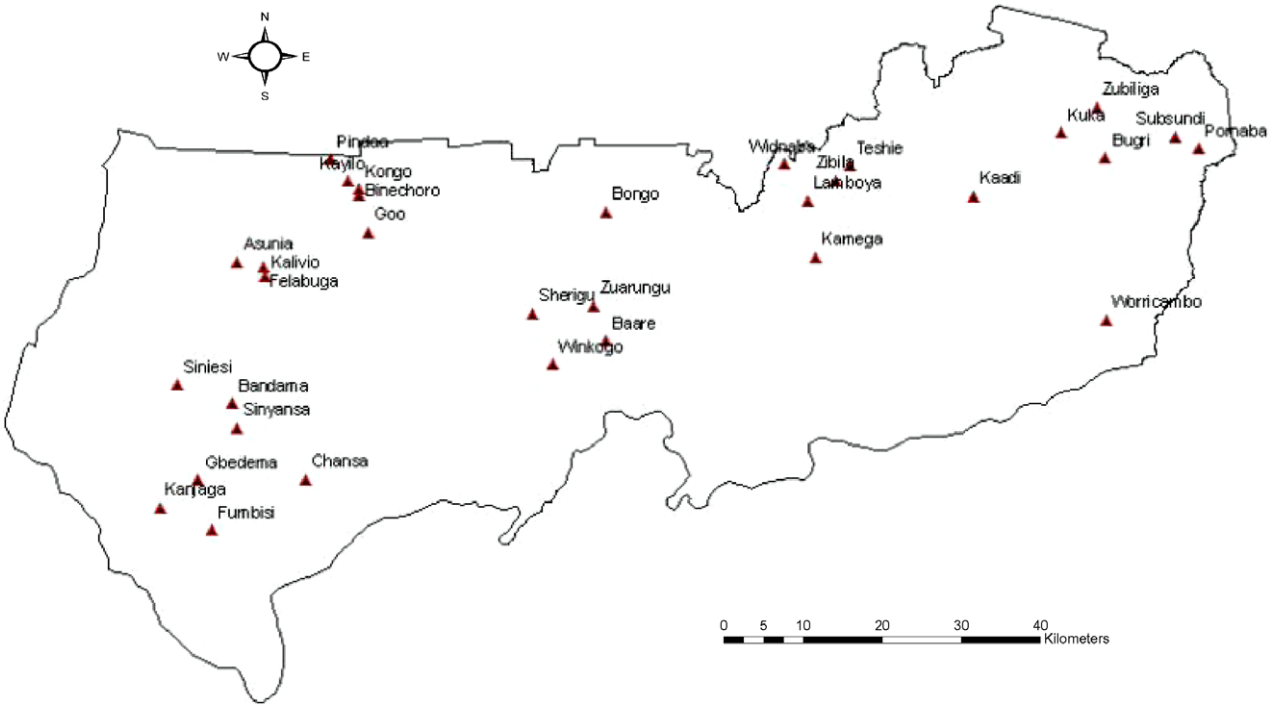

Fig. 3. Map showing the locations of dams visited during field work in the UER, January–February 2007.

Fig. 4. Winkogo dam with reeds on the surface of the reservoir.

$$\mathrm{NDAI} = \frac{(\mathrm{Area}_{\mathrm{field}} - \mathit{Area}_{\mathrm{sat}})}{(\mathit{Area}_{\mathrm{field}} + \mathit{Area}_{\mathrm{sat}})} \quad (2)$$

$$\mathrm{DAI} = \frac{(\mathit{Area}_{\mathrm{field}} - \mathrm{Area}_{\mathrm{sat}})}{\mathrm{Area}_{\mathrm{field}}} \quad (3)$$

The NDAI value lies between −1 and 1 with values close to zero giving the best linear fit between the surface areas obtained from field and satellite. Values increasing to both extremes indicate increasing deviation between $\mathrm{Area}_{\mathrm{field}}$ and $\mathrm{Area}_{\mathrm{sat}}$. A negative value implies that $\mathrm{Area}_{\mathrm{field}} < \mathrm{Area}_{\mathrm{sat}}$ and vice versa. Sawunyama et al. (2005) expressed the difference between $\mathrm{Area}_{\mathrm{field}}$ and $\mathrm{Area}_{\mathrm{sat}}$ as a fraction of the field area. The DAI values also lie between −1 and 1, with values close to 0 giving the best linear fit between field area and satellite area, values increasing to both extremes indicates increasing deviation between $\mathrm{Area}_{\mathrm{field}}$ and $\mathrm{Area}_{\mathrm{sat}}$. A negative value implies that $\mathrm{Area}_{\mathrm{field}} < \mathrm{Area}_{\mathrm{sat}}$ and vice versa.

The results obtained from the DAI and NDAI show that there is a very good linear fit between the two data sets. A linear regression between $\mathrm{Area}_{\mathrm{field}}$ and $\mathrm{Area}_{\mathrm{sat}}$ gave at 95% confidence interval ($p < 0.05$), a Pearson correlation coefficient (r^2) of 0.9 when the intercept of the trend line was set to zero. As shown in Fig. 5 the correlation between the field area and satellite is given by

$$\mathrm{Area}_{\mathrm{field}} = 0.93\mathrm{Area}_{\mathrm{sat}} \quad (4)$$

Eq. (4) implies that the satellite images overestimated the areas of the reservoirs by about 7% compared to ground measurements. Fig. 5 shows that on the average the difference between the satellite-derived surface areas and that obtained from ground measurements decreased with increasing surface area of reservoirs. This difference may be due to over-estimation of the water surface. The flat and smooth surfaces surround the reservoirs may be difficult to distinguish from water. A more important and more likely explanation is the simple fact that the ground survey took place after the image acquisition, with a lag of a few days to two weeks. Because the study period coincided with the dry period during which evaporation and irrigation are maximal, the lag causes a decrease in water area in the reservoirs.

Table 2
Comparison of water surface area of reservoirs as measured in field and with satellite data

S/N	Reservoir	Coordinates UTM_Zone_30 N		$Area_{sat}$ (ha)	$Area_{field}$ (ha)	DAI	NDAI
		Easting	Northing				
1	Asunia	688519	1199713	1.83	2.07	0.12	0.06
2	Baare	741393	1188174	9.46	8.4	−0.13	−0.06
3	Binechoro	705991	1209490	2.37	3.82	0.38	0.23
4	Bugri	813102	1214561	9.78	10.86	0.1	0.05
5	Dua	742458	1205006	5.07	4.55	−0.11	−0.05
6	Kalivio	692806	1197731	1.65	2.91	0.44	0.28
7	Kamega	771437	1200195	10.21	11.07	0.08	0.04
8	Kongo	705806	1210086	6.9	5.98	−0.15	−0.07
9	Lamboya	770624	1208052	20.71	20.08	−0.03	−0.02
10	Pornaaba	826129	1216427	27.43	23.92	−0.15	−0.07
11	Sherigu	730791	1192574	3.82	4.42	0.14	0.07
12	Teshie	776191	1213188	4.34	3.39	−0.28	−0.12
13	Widenaba	767072	1213463	7.32	6.56	−0.11	−0.05
14	Winkogo	734066	1185119	0.81	3.66	0.78	0.64
15	Worricambo	813451	1191313	14.25	11.38	−0.25	−0.11
16	Yirdongo	743415	1213303	15.83	14.15	−0.12	−0.06
17	Zebila	774862	1211115	5.24	10.86	0.52	0.35
18	Zuarungu	739805	1193383	1.03	1.43	0.28	0.16

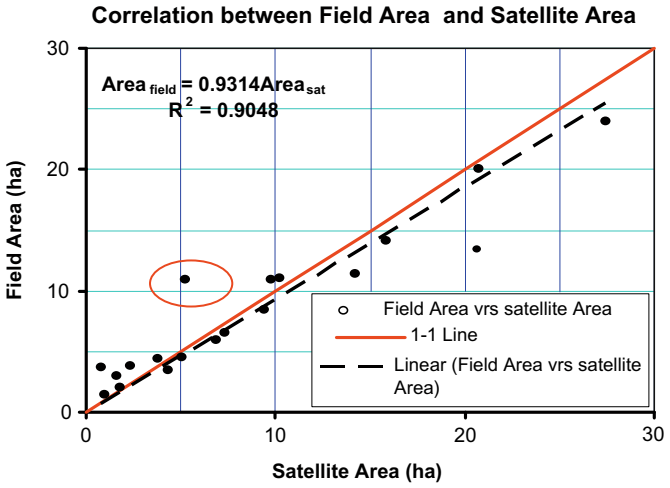

Fig. 5. Correlation between field surface area and satellite area. The point circled is Zebila reservoir.

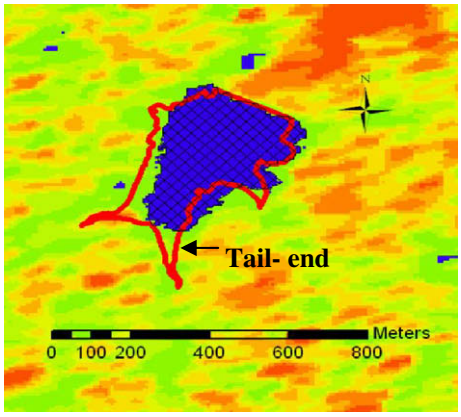

Fig. 7. Under classified Kamega reservoir.

An example of an over classified water boundary is shown in Fig. 6. The shaded area (dark) is the area classified as water in the satellite image and the area enclosed within the polygon is the outline obtained from the field. The light coloured areas are vegetation. The area below the dam wall (yellow line in Fig. 6) is a farmland and therefore appears bright.

From Table 2 it can be seen that despite the general over-classification of water surfaces by satellite images, in some cases the satellite images under-estimated the water surface area ($Area_{field} > Area_{sat}$). This is exemplified by Zebila reservoir, indicated in Fig. 5 as the circled point, where the satellite estimate was almost half

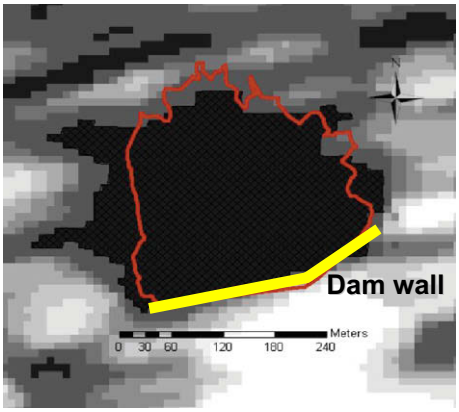

Fig. 6. Over-classified Kongo reservoir. (For interpretation of the references to colour in this figure legend, the reader is referred to the web version of this article.)

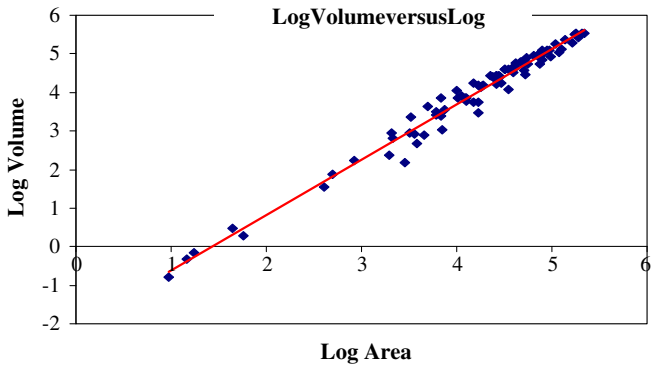

Fig. 8. Graph indicating the correlation between reservoir volumes and their corresponding surface areas.

Table 3
Volume of reservoir estimated from satellite imagery

S/N	Name of Reservoir	$Area_{sat}$ (ha)	Estimated $Area_{field}$ (ha)	Estimated actual stored water volume $\times 10^4$ m^3
1	Asunia	1.83	1.7	1.08
2	Baare	9.46	8.81	11.56
3	Binechoro	2.37	2.21	1.58
4	Bugri	9.78	9.12	12.15
5	Dua	5.07	4.72	4.70
6	Kalivio	1.65	1.53	0.93
7	Kamega	10.21	9.52	12.92
8	Kongo	6.9	6.43	7.34
9	Lamboya	20.71	19.3	35.74
10	Pornaaba	27.43	25.56	53.57
11	Sherigu	3.82	3.56	3.13
12	Teshie	4.34	4.04	3.76
13	Widenaba	7.32	6.82	7.99
14	Winkogo	0.81	0.76	0.34
15	Worricambo	14.25	13.28	20.86
16	Yirdongo	15.83	14.75	24.27
17	Zebila	5.24	4.88	4.94
18	Zuarungu	1.03	0.96	0.47

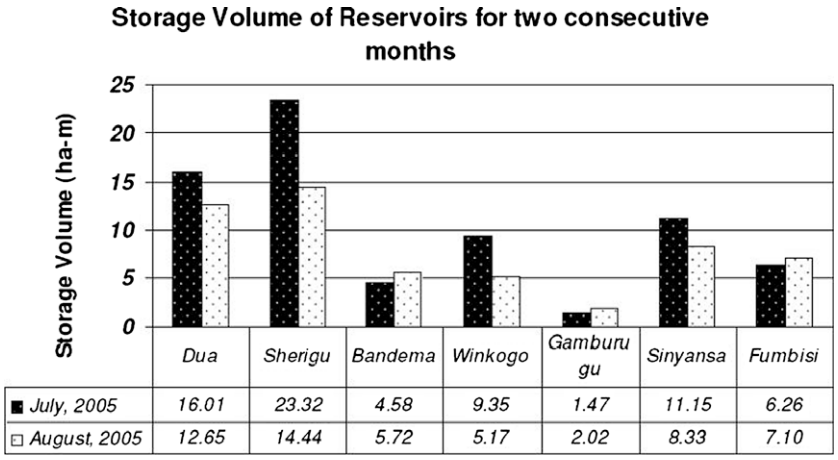

Fig. 9. Reservoir storage in July and August, 2005.

of that obtained from the field. This was due to the fact that there were reeds/dense vegetation on the surface of this reservoir. If these reeds were located in the middle of the reservoir, as it occurred in some reservoirs, it would not have had much influence since that area would still have been identified to be part of the reservoir. In cases where the reeds were at the tail-end or at the edges these were often classified as land/vegetation and not water. This was also the case with Winkogo reservoir with many reeds on its surface (Fig. 4) of which, as a consequence, about 78% of the water was classified as land/vegetation. Another example of a reservoir where $Area_{field} > Area_{sat}$ is shown in Fig. 7. The shaded area (dark) is the area classified as water in the satellite image and the area enclosed within the polygon is the outline obtained from the field. The areas at the tail-end of the reservoir are classified as vegetation instead of water.

4.2. Surface area–volume correlation

If reservoirs can be assumed to approximate the shape of a square pyramid diagonally cut in half (Liebe, 2002), the area–volume relation will have the following relation

$$V = a^{*}\mathrm{Area}^{b} \tag{5}$$

where V is the volume of the reservoir, and a and b constants. If reservoirs are indeed exactly half pyramids, then $b = 1.5$. When the slopes are more convex (rare), $b > 1.5$. In the more common case of concave slopes, $b < 1.5$. The values of a and b are surprisingly constant within geomorphologically similar areas. Eq. (4) was parameterized by using the 3-D reservoirs models, giving the area–volume correlation shown in Fig. 8. The corresponding equation, with an r^2 value of 98%, is

$$V = 0.00875^{*}\mathrm{Area}^{1.44}(m^3) \tag{6}$$

A study carried out in the upper east of Ghana by Liebe et al. (2005) found a similar correlation between the surface area of reservoirs and their storage volume, based on bathymetrical measurements carried out in 2002, as follows

$$\mathrm{Volume}_{reservoir} = 0.00857\mathrm{Area}_{sat}^{1.4367}(m^3) \tag{7}$$

It can be seen that Eq. (6) is not very different from Eq. (7) which implies that the correlation between reservoir areas and volumes is robust and can be reproduced over time. Eqs. (4) and (6) were then used to estimate the actual volume of water stored in the reservoirs. The resulting surface areas and volumes were named Estimated Areafield. The results are presented in Table 3.

4.3. Monthly inventory of storage in reservoirs

Two ENVISAT ASAR satellite images captured during the rainy season (14th July, 2005 and 18th August, 2005) were used to deter-

mine the volume of water stored in seven selected reservoirs for two consecutive months. The result is presented in Fig. 9. It must however be noted that it is not easy to monitor the reservoir volume over the dry period as the contrast between land and water becomes less.

An explanation for the varying percentage change in volume from reservoir to reservoir was beyond the scope of this research, but may be related to natural variations in inflow into the reservoirs and different seepage and other water losses due to leakage. Fig. 9 shows clear differences between stored volumes measured over a period of approximately one month, which means that with the help of radar images reservoirs could be monitored regularly, all year-round.

5. Conclusions

The following specific conclusions may be drawn:

(1) There is a good linear correlation between the wetted surface areas of reservoirs obtained in the field and those from satellite (radar) images.
(2) All year-round regional monitoring of actual storage volume in reservoir in the upper east region in Ghana is feasible using radar-based remote sensing and GIS.
(3) Reeds, which can be found in the shallow tail-ends of reservoirs, are not readily distinguishable from the surrounding vegetation by Envisat ASAR imagery.
(4) In general, HH polarization seems the best combination of polarizations to use, although sometimes HV gives better results, depending on wind conditions.
(5) Although dual polarization of the SLC ENVISAT ASAR is optimal, it is less useful to combine C-HH and C-HV channels especially in cases where one is good and the other bad. A combination does not enhance the land/water contrast compared to using only one channel.
(6) Due to the fact that the volume of water can be easily estimated on a monthly basis using radar imagery, the results obtained can be used as inputs in water allocation and water resources planning models. This can enhance the quality of decision making.
(7) Remote sensing is a rapid and cost-effective way of obtaining information at relatively low temporal and high spatial resolutions. Costs are low when compared to traditional methods of ground survey, which is time consuming and labour intensive. Nevertheless, remote sensing requires a high start up cost in terms of training experts to use GIS and remote sensing application software, computer hardware requirements and acquisition of satellite images. Remote sensing and GIS can, to a large extent, overcome the difficulty in the collection, transfer and sharing of data. The use of these technologies will enhance the efficient management of reservoirs for crop productions and help reduce poverty in semi-arid environments.

Acknowledgement

Assistance by the GLOWA-Volta (<http://www.glowa-volta.de>), the small Reservoirs Project (<http://www.smallreservoirs.org>), and by the water resources Environment and Sanitation Project at Kwame Nkrumah University of Science and Technology, Kumasi, Ghana, is very much appreciated. ESA's Tiger Project (AO2871, <http://tiger2871.shorturl.com>) provided the radar images used in this research.

References

Balazs, C., 2006. Rural Livelihoods and Access to Resources in Relation to Small Reservoirs: a study in Brazil's Preto River Basin. MSc. thesis, University of California, Berkeley, Ca.

Faulkner, Joshua, W., Steenhuis, Tammo, Giesen, Nick van de, Andreini, Marc, Liebe, Jens R, 2008. Water use and productivity of two small reservoir irrigation schemes in Ghana's upper east region. Irrigation Drain. 57, 151–163.

Frost, V.S., Stiles, J.A., Shanmugan, K.S., Holtzman, J.C., 1982. A model for radar images and its application to adaptive digital filtering of multiplicative noise. Institute of electrical and electronics engineers Inc., (IEEE).. Transactions on Pattern Analysis and Machine Intelligence PAMI 4 (2), 157–166.

GPRSP (2005). Ghana poverty reduction strategy paper II – 2006–2009. National report. (Available from <http://siteresources.worldbank.org/INTPRS1/Resources/Ghana_PRSP>(Nov-2005).pdf) (Accessed online: 11/03/07).

Gyau-Boakye, P., Tumbulto, J.W., 2006. Comparison of rainfall and runoff in the humid south–western and the semiarid northern savannah zone in Ghana. African Journal of Science and Technology 7 (1), 64–72.

Herold, N.D., Haack, B.N., Solomon, E., 2004. An evaluation of radar texture for land use/cover extraction in varied landscapes. International Journal of Applied Earth Observation and Geoinformation 5, 113–128.

Horritt, M.S., Mason, D.C., 2001. Flood boundary delineation from synthetic aperture radar imagery using a statistical active contour model. International Journal of Remote Sensing 22 (13), 2489–2507.

IFAD (2007). Ghana: upper east region land conservation and smallholder rehabilitation project (LACOSREP), report. (Available at <http://www.ifad.org/evaluation/public_html/eksyst/doc/prj/region/pa/ghana/s026ghbe.htm>) (Accessed online: 12/03/07).

Liebe, J., 2002. Estimation of Water storage capacity and evaporation losses of small reservoirs in the upper east region of Ghana. Diploma thesis, University of Bonn, Germany.

Liebe, J., van de Giesen, N., Andreini, M., 2005. Estimation of small reservoir storage capacities in a semi-arid environment: a case study in the upper east region of Ghana. Physics and Chemistry of the Earth 30, 448–454.

Mialhe, F., Gunnell, Y., Mering, C., 2008. Synoptic assessment of water resource variability in reservoirs by remote sensing: general approach and application to the runoff harvesting systems of south India. Water Resources Research 44. doi:10.1029/2007WR006065. W05411.

Poolman, Martine, I., van de Giesen, N.C., 2006. Participation; rhetoric and reality. The importance of understanding stakeholders based on a case study in upper east Ghana. International Journal of Water Resources Development 22 (4), 561–573.

Sawunyama, T., Senzanje, A., Mhizha, A., 2005. Estimation of small reservoir storage capacities in Limpopo River Basin using geographical information systems (GIS) and remotely sensed surface areas: case of Mzingwane catchment. Physics and Chemistry of the earth 31 (15), 935–943.

Toyra, J., Pietroniro, A., Martzl, L.W., Prowse, T.D., 2002. A multi-sensor approach to wetland flood monitoring. Hydrological Processes 16, 1569–1581.

Van de Giesen, N., (2000). Characterization of West African shallow flood plains with L- and C-band radar in remote sensing and hydrology 2000 (Proceedings of a symposium held at Santa Fe, New Mexico, USA, April 2000). IAHS 267.

Xu, K., Zhang, J., Watanabe, M., Sun, C., 2004. Estimating river discharge from very high-resolution satellite data: a case study in the Yangtze River China. Hydrological Processes 18, 1927–1939.